Nuclear Science and Techniques (2023) 34:19
https://doi.org/10.1007/s41365-023-01180-9

Efficient and selective extraction of uranium from seawater based on a novel pulsed liquid chromatography radionuclide separation method

Jian-Hua Ye[1,2,3] · Tao Yu[1,2,3]

Received: 8 September 2022 / Revised: 8 November 2022 / Accepted: 14 November 2022 / Published online: 20 February 2023

Abstract

The novel pulsed liquid chromatography radionuclide separation method presented here provides a new and promising strategy for the extraction of uranium from seawater. In this study, a new chromatographic separation method was proposed, and a pulsed nuclide automated separation device was developed, alongside a new chromatographic column. The length of this chromatographic column was 10 m, with an internal warp of 3 mm and a packing size of 1 mm, while the total separation units of the column reached 12,250. The most favorable conditions for the separation of nuclides were then obtained through optimizing the separation conditions of the device: Sample pH in the column = 2, sample injection flow rate = 5.698 mL/min, chromatographic column heating temperature = 60 °C. Separation experiments were also carried out for uranium, europium, and sodium ions in mixed solutions; uranium and sodium ions in water samples from the Ganjiang River; and uranium, sodium, and magnesium ions from seawater samples. The separation factors between the different nuclei were then calculated based on the experimental data, and a formula for the separation level was derived. The experimental results showed that the separation factor in the mixed solution of uranium and europium (1:1) was 1.088, while achieving the initial separation of uranium and europium theoretically required a 47-stage separation. Considering the separation factor of 1.50 for the uranium and sodium ions in water samples from the Ganjiang River, achieving the initial separation of uranium and sodium ions would have theoretically required at least a 21-stage separation. Furthermore, for the seawater sample separation experiments, the separation factor of uranium and sodium ions was 1.2885; therefore, more than 28 stages of sample separation would be required to achieve uranium extraction from seawater. The novel pulsed liquid chromatography method proposed in this study was innovative in terms of uranium separation and enrichment, while expanding the possibilities of extracting uranium from seawater through chromatography.

Keywords Pulsed liquid chromatography · Nuclide separation · Seawater uranium extraction · Uranium enrichment

1 Introduction

Uranium extraction from seawater is strategically important in guaranteeing the sustainable development of nuclear energy and ensuring successful completion of China's carbon peak and carbon-neutral goals. As an efficient and clean energy source, nuclear power is gradually becoming a more important factor in China adjusting its energy structure,

This work was supported by the Natural Science Foundation of Jiangxi Province, China (No. 20202BABL203004), the Opening Project of the State Key Laboratory of Nuclear Resources and Environment (East China University of Technology)(No. 2022NRE23), and the Opening Project of Jiangxi Province Key Laboratory of Polymer Micro/Nano Manufacturing and Devices (No. PMND202101).

✉ Tao Yu
xiaoshan770@163.com

[1] State Key Laboratory of Nuclear Resources and Environment, East China University of Technology, Nanchang 330013, China

[2] Jiangxi Province Key Laboratory of Polymer Micro/Nano Manufacturing and Devices, East China University of Technology, Nanchang 330013, China

[3] School of Nuclear Science and Engineering, East China University of Technology, Nanchang 330013, China

achieving coordinated economic and environmental development, and promoting industrial structure upgrades [1, 2]. Uranium is a key resource and forms the basis for the development of nuclear energy, although the existing terrestrial uranium reserves are relatively poor and are only expected to be sufficient for human use for approximately 100 more years. In contrast, seawater contains more than 4.5 billion tons of uranium, almost 1000 times greater than the amount of terrestrial uranium reserves; thus, seawater uranium extraction is expected to be a feasible solution for ensuring the sustainable development of nuclear energy [3, 4]. In addition, to satisfy China's commitment to achieve "peak carbon" by 2030 and to be "carbon neutral" by 2060, the proportion of nuclear power in China's total electricity needs to be increased further. This will require a higher demand for a diversified and sustainable supply of uranium resources. Research on uranium extraction from seawater has been conducted for several decades, and this was primarily focused on two aspects. Firstly, in methodological studies, mainly adsorption [5–10], extraction [11, 12], precipitation [13, 14], ion exchange [15], electrochemical extraction [16, 17], photocatalysis, etc. [18, 19], and bioconversion [20, 21]; secondly, in materials research, mainly focused on the preparation and study of adsorbent materials and extractants. For example, Das, Sadananda et al. synthesized polymeric fiber-based adsorbents, aminooxane macroporous membranes, and other materials through radiation-induced graft polymerization and subsequently used these for uranium extraction from seawater, considering that these materials had a high adsorption capacity and faster adsorption kinetics for uranium [22, 23]. Furthermore, Salam et al. synthesized a new cationic surfactant (GCS) for the extraction and separation of sulfate solutions from U(VI) ions [24]. Adsorption is the most widely used method for uranium extraction from seawater owing to its simplicity of operation. Inorganic, polymeric, and nanostructured materials, as well as biomaterials, have been previously used to prepare seawater uranium adsorbents. Among these, the amidoxime group (AO) adsorbent has advantages such as simple preparation, high physical and chemical stability, and strong coordination binding with uranium at the pH of seawater (8.3). Moreover, amidoxime group adsorbents have already been used in large-scale engineering tests around the beginning of the century, thus proving their practicality [25–27]. Similarly to inorganic adsorbents, they also have a low cost, large specific surface area, adjustable pore structure, and easy preparation. However, they are mostly in a powdered form, are difficult to recover, and presently are still in the laboratory research stage. Nanosorbents have advantages such as a high specific surface area, high adsorption site density, and rapid mass transfer, although their technology is still developing and they are difficult to prepare in bulk. Polymer adsorbents have high strength, good flexibility, an adjustable molecular structure, and are easy to mass produce; however, this material is costly and vulnerable to the marine environment. The main advantages of microbial adsorbents include their fast adsorption rate, good selectivity, and low cost, yet they are difficult to control and unsuitable for high-concentration UO_2^{2+} wastewater [28, 29]. The extraction method used for uranium separation plays an important role in hydrometallurgy, reprocessing, and the treatment of uranium in uranium-containing wastewater. The extractant holds the most significant role in the extraction process, and currently, the main uranium extractants are tributyl phosphate (TRPO) and trialkylphosphine oxide [30]. Recent research has been mainly focused on new extractants, such as phthalamides, aluminescents, macrocyclic compounds, and ionic liquids [31, 32]. Membrane extraction, also known as fixed-membrane interface extraction or membrane-based solvent extraction, is a novel method that has unique advantages. These include the fact that the membrane extraction mass transfer process occurs on the microporous membrane surface or in the pore channel, which can reduce the entrapment loss of extractant in the feed-liquid phase, reducing the physical requirements of extractant, broadening the range of extractant selection, and avoiding the influence of "re-mixing" phenomenon in the extraction process. The extraction process also breaks the limitation of the "liquid flooding" condition and can use a very high water–oil ratio [33]. Solid phase extraction (SPE) plays an increasingly important role in the separation and analysis of key nuclides such as uranium, especially in the treatment of uranium contamination in various environmental waters, owing to its high enrichment factor, relatively high operational flexibility and irradiation stability, fast sorption kinetics, reusable extractants, low consumption of organic reagents, low waste generation, and easy solidification of failed materials [34]. Photocatalysis is another hot topic in research on seawater uranium extraction. Photocatalytic reactions have been widely used for CO2 reduction, water decomposition, heavy metal treatment, organic pollutant degradation, and photosynthesis, and can adjust the valence state of metal ions over a wide range without requiring other reducing agents or electric fields. During photocatalytic reduction, U(VI) in water was effectively reduced and removed [35, 36]. In seawater, the photocatalytic method can achieve an extraction of 3960 mg/g in just a few hours with a simple and efficient elution of the extracted uranium [35]. In addition, photocatalysis has high selectivity for U(VI) in the presence of multiple coexisting ions [36, 37]. The photocatalytic extraction of uranium from aqueous solutions has advantages such as a high extraction capacity, high selectivity, and fast kinetics, all of which are superior to those of other methods, as shown in Table 1.

Presently, the use of chromatography for uranium extraction from seawater is relatively rare [44]. In the past, the performance of chromatographic separation has

Table 1 Comparison of the efficiency of photocatalytic materials in the literature

Materials	pH top value	Efficiency	Light reaction time	Uranium content	References
Bi_2 WO_6	6.5	53%	600 min	30 mg/L	[38]
ZnO/TiO2–SiO2	5.5	97%	240 min	47 mg/L	[39]
Carboxylated g-C_3N_4	8.2	100%	50 min	27 mg/L	[40]
TiO_2	5.0	50–100%	180 min	27 mg/L	[41]
Te@O–SnS_2	4.8	97.3%	60 min	8 mg/L	[42]
$ZnFe_2O_4$	5.0	95%	40 min	50 mg/L	[43]

been largely dependent on the type and nature of the stationary phase. However, the differences in the properties of the solution components themselves and the mechanisms of their interaction with the stationary phase were neglected, and thus, have been greatly limited in dealing with the separation of complex systems such as seawater. Research focused on chromatographic stationary phases with high selectivity and separation performance is the main driver for the development of chromatographic techniques.

Therefore, this study is based the mechanisms and methods of uranium extraction from seawater, with the context of national strategic requirements. Herein, the problems and shortcomings of traditional methods are addressed, including adsorption and extraction, which are costly, complicated, and time-consuming, the separation requirements to reach the equilibrium of adsorption and extraction, and the inability to achieve dynamic separation. A dynamic chromatographic separation method was used here to achieve rapid separation of uranium in a non-equilibrium state. The key aims of this study were (1) to establish a pulsed liquid chromatographic nuclide separation device and to construct a chromatographic separation system consisting of six components to achieve pulsed automatic sample feeding, automatic separation, and online automatic detection. (2) to determine the separation factors and steps of this method by testing optimal separation conditions and conducting research on the separation conditions and mechanisms of nuclide chromatography. The effects of varying column fillings, sample flow rates, pH levels, heating and cooling temperatures, and types and concentrations of coexisting ions on the separation effect were all investigated. Furthermore, the kinetic and thermodynamic mechanisms under these various conditions were explored. (3) Laboratory studies on seawater uranium extraction were then carried out under the optimal experimental conditions and at the most suitable separation levels to determine the effectiveness of the separation devices, verify the correctness of the separation principles and the economy of the methods, and to provide new feasible methods and ideas for seawater uranium extraction.

2 Experimental section

2.1 Instruments and reagents

The instruments required for this study included a new self-developed chromatographic column and switching pulse injection device, modified 721 online spectrophotometric detector, peristaltic pump with model BQ80S + FZ10-CE, 85–2 digital display temperature-controlled magnetic stirrer, inductively coupled plasma mass spectrometer (ICP-MS) with model Agilent 7500cx, and inductively coupled plasma emission spectrometer (ICP-OES) with model iCAP7400. The experimental reagents and samples used in this study were pH = 1 HCl as the elution liquid, pH = 2 HCl as the mobile phase, treated Ganjiang River water samples, seawater samples, varying concentrations of europium and uranium solutions, and varying concentrations of cation solutions.

2.2 Preparation of a new chromatographic column

The column used for the experiments in this study was constructed to be 10 m long rubber tube, with a 5 mm outer diameter, and 3 mm inner diameter as the column body and 1 mm diameter adsorbent beads as fillers, with glass tube joints connected to each end of the rubber tube and sand cores inside the joints, which were used with characteristics such as high strength, acid resistance, and reusability. It was calculated that 0.82 mm in the column was equivalent to one separation unit, while the total separation units could reach 12,250. Before preparation, the filling and tube body were cleaned using dilute hydrochloric acid, followed by ethanol, and then distilled water. The column was then loaded using the wet method after drying. The separation principle of this column used the differences in the masses of elements to achieve separation: quantum separation. As shown in Fig. 1:

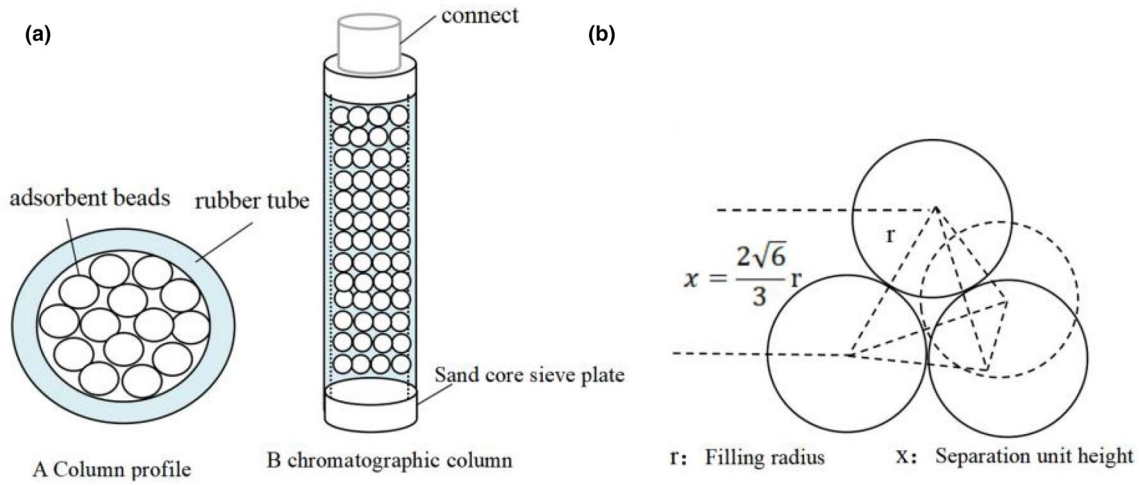

Fig. 1 (Color online) Schematic diagram of the chromatographic column (**a**), separation unit (**b**)

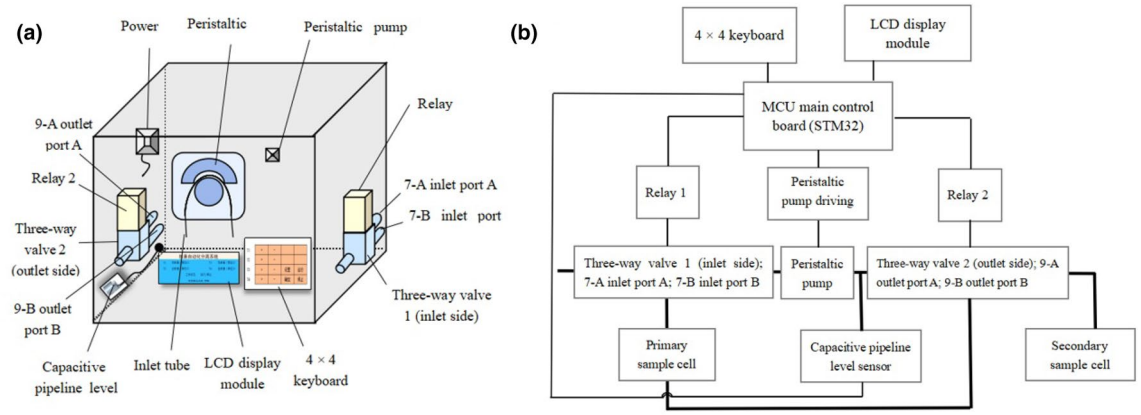

Fig. 2 (Color online) Schematic diagram of the switching pulse feeder (**a**) Schematic diagram of the electronic control (**b**)

2.3 Switching pulse injection device design

The switching pulse injection device consisted of two parts: Pulse generation and control of the solution feed and separation, which is illustrated in Fig. 2a, b. Pulse action is the decisive factor in achieving the sustainable separation of nuclides, with each pulse in the sample being separated. The pulses were generated in such a way that the column first entered the air at T1 time, the solution at T2 time, and then the air at T1 time at the end of T2 time, and so on, to generate a pulse injection. When the device automatically recognized that the incoming solution was coming out of the chromatographic column, T3 began timing. T3 was the optimal shunt time, and at the end of T3, the device collected the samples coming out of the column individually to achieve separation. The control of sample separation in the column was key in achieving nuclide separation, while the time setting of separation action was directly related to the effect of nuclide separation.

2.4 Establishment and application of pulsed liquid chromatography system for nuclide separation

A pulsed liquid chromatography nuclide separation device was established to achieve nuclide separation based on precise spatial and temporal control. There were six components of this nuclide separation device: The chromatographic cycle separation system, mainly composed of chromatographic columns for chromatographic separation, the switching pulse injection system, a device to generate injection pulses, the time-controlled automatic shunting system, mainly used to monitor and control sample shunt, and was a control device to realize automatic nuclide separation, and the online detection and analysis system, a system for real-time detection of product composition

and verification of separation effect. Unlike the physical nuclide detection device principle [45, 46], this device used ICP-MS to detect and analyze the nuclides coming out of the column in real time, and controlled the nuclide separation by sending analysis results to the time-controlled automatic shunting system. There was also the adjustable flow system, which was the power source of the entire system and the automatic control system, an auxiliary device to control the interaction between nuclides and fillers. Among these, the chromatographic cycle separation system was the core of the device, while the other five systems responded to it and were linked by connecting devices. This is shown in Fig. 3.

The sample solution to be separated and concentrated was added to the cuvettes and a switching pulse feed system was then used to drive the connecting pipeline between the inlet end of the column and one of the cuvettes. The sample solution was delivered to the column in pulsed mode using the timed automatic switching inlet as the source of the pulsed flow. The sample entered the column, and after separate blocking action, the nuclide was separated from other interfering particles, and the sample subsequently exits the column. At the exit end of the column, the fluid flow direction was controlled by a time-controlled automatic shunt system; the first part of the sample containing less uranium flowed back to the primary cuvette through the reflux tube, while the latter part of the sample containing more uranium flowed to the second sample/sub-cuvette to wait for the next level of separation and concentration. The separation and concentration of nuclides could then be achieved by repeating this several times.

3 Results and discussion

3.1 Determination of optimum conditions for the separation of uranium solutions through a chromatographic column

To determine the optimal conditions for chromatographic separation, experimental studies on the over-column acidity, over-column flow rate, heating and cooling bath temperatures, pulse feed method (amount of sample per pass and pulse interval time), coexisting ions, and shunting time were required.

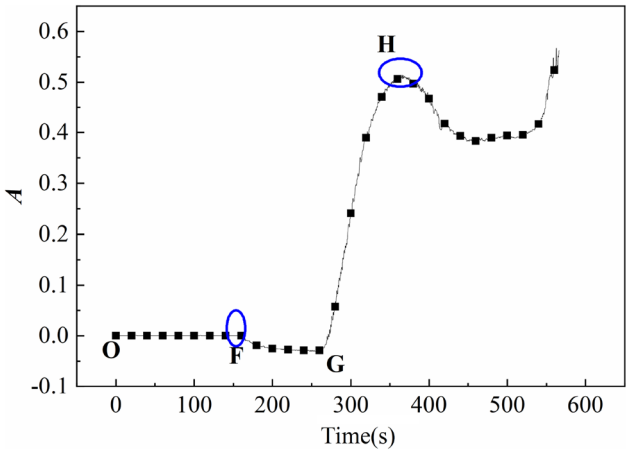

Fig. 4 Variation in uranium separation within the chromatographic column

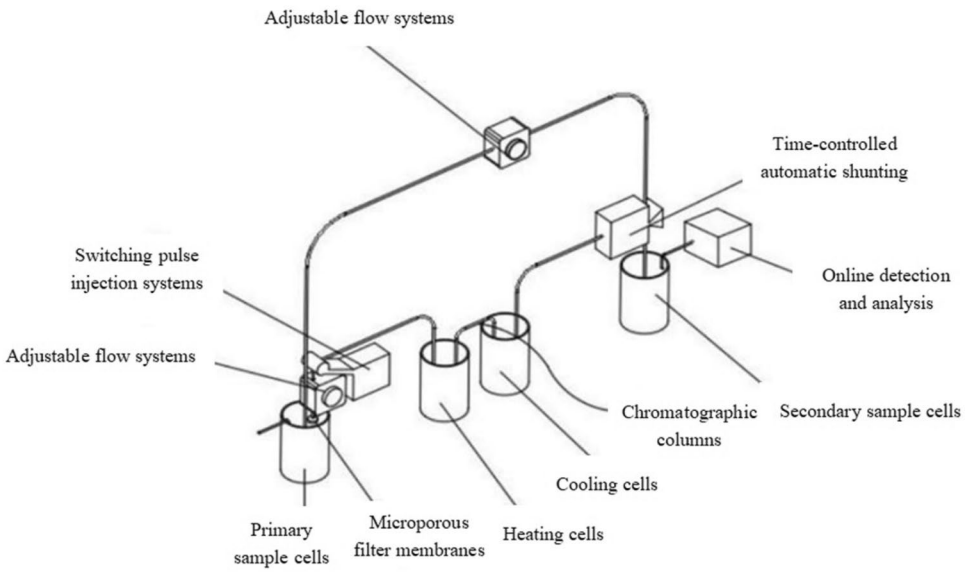

Fig. 3 Schematic diagram of nuclide chromatography separation system

3.1.1 Graph of uranium separation variation within the chromatographic column

The experiment required 30 mL of uranium solution in the column, with the uranium-containing solution exiting through the column, which developed color with an azoarsine III chromogenic agent being placed into the detector (online spectrophotometer). A set of images were taken after color development on the detector, and the change in the curve was equal to the change in uranium concentration after the reaction exited the column, which was reflected by the absorbance value. As shown in Fig. 4, point O was the time at which the sample entered the column, point F was the time at which the sample exited the column (150 s), the absorbance of the OF section was the value after the chromogenic agent was zeroed, and point G was the time at which the uranyl ion in the sample exited (270 s). After the sample exited the FG section, the chromogenic agent was diluted, the absorbance decreased, and there were almost no uranyl ions in this section of the solution. The absorbance increased after point G, and this change in absorbance allowed monitoring of the changes in uranium within the column. Point H was the time at which uranium was at its highest concentration, that is, the peak time. The fluctuation after the peak was caused by pulse injection, which resulted in a better separation between the nuclides that had reached the peak and those that had not yet reached the peak during the separation of multiple nuclides.

3.1.2 Effect of pH on the separation of uranium and europium

The sample acidity across the column was one of the most important factors in determining ion movement and separation status. In solution, with a decrease in hydrogen ions (pH increase), the filler surface underwent protonation and deprotonation, which was reflected in the change in the surface potential of the filler. Considering that the purpose of this study was to slow down the movement of uranyl ions through the action of the filler and its liquid film, rather than adsorbing uranyl ions on the filler surface, the separation of nuclides was typically selected at a low pH (pH < 3) stage. The separation of uranium and europium mixed solutions in the column at different pH values was then measured by adding 15 mL each of the same concentrations of uranium and europium into the column with a sample injection flow rate of 3.802 mL/min. In the 30 mL sample solution, the first 7 mL sample solution in the column was discarded because of the low ion concentration, as shown in the FG segment of Fig. 4. Therefore, the last 21 mL of the sample solution was collected, with every 3 mL of solution comprising one sample. The test results are shown in Fig. 5. Figure 5a shows the concentration variation of uranyl ions at different pH levels, while Fig. 5b shows the concentration variation of europium ions at different pH values, which were detected and analyzed by ICP-OES. The results of this showed that the concentration of uranyl ions exiting chromatography was highest at pH = 2 for uranium solutions, i.e., the highest separation concentration; separation concentration was highest for europium solutions at pH = 0.1.

Figure 6a shows the separation of uranium and europium mixed solution at pH = 0.1, while Fig. 6b shows the separation of uranium and europium mixed solution at pH = 1, and Fig. 6c shows the separation of uranium and europium mixed solution at pH = 2. Comparing these three cases, at pH = 0.1 and pH = 1, the column had a lesser effect on the separation hindrance effect of uranium and europium, which led to a uniform change in the concentration of uranium and europium exiting the column, and the separation here was poor. When pH = 2, the concentration difference between uranium and europium exiting the column was the largest, that is, the separation was greatest. Therefore, pH 2 was chosen as the acidity of the experimental sample passing through the column.

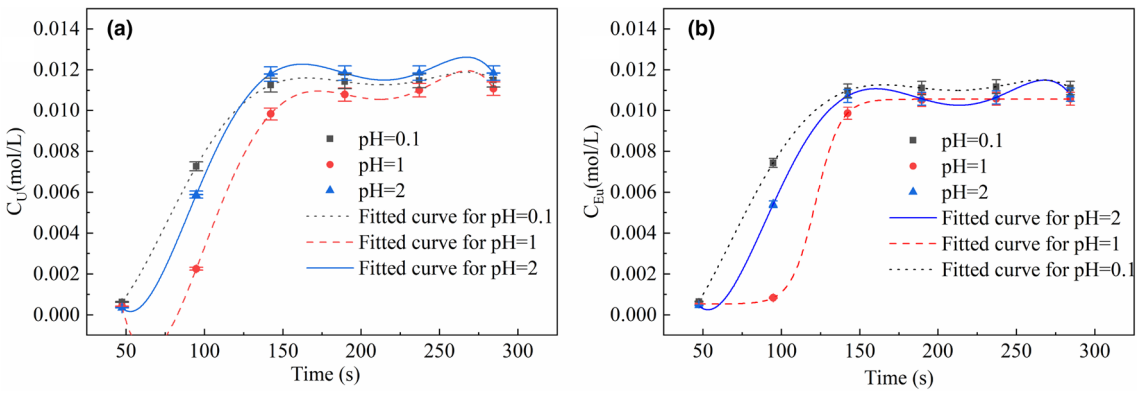

Fig. 5 (Color online) Diagram of the separation of the same element in mixed solutions at different pH levels. Uranium (**a**); europium (**b**)

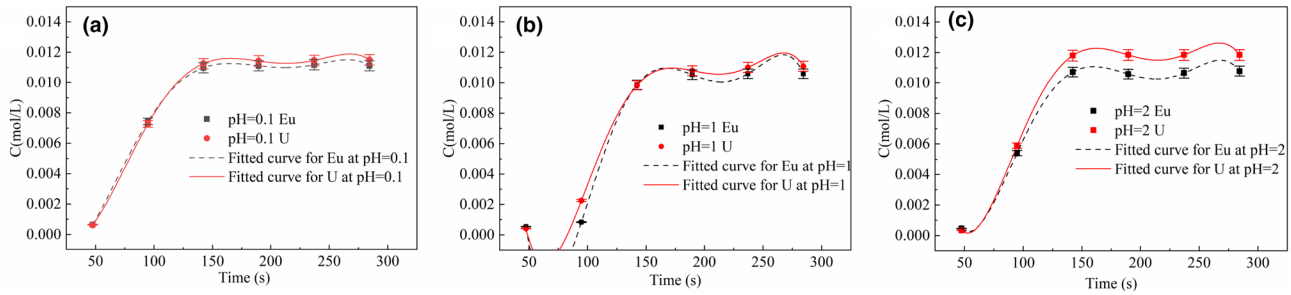

Fig. 6 (Color online) Plots of the separation of uranium and europium in mixed solutions at the same pH level. **a** mixed solution pH = 0.1; **b** mixed solution pH = 1; **c** mixed solution pH = 2

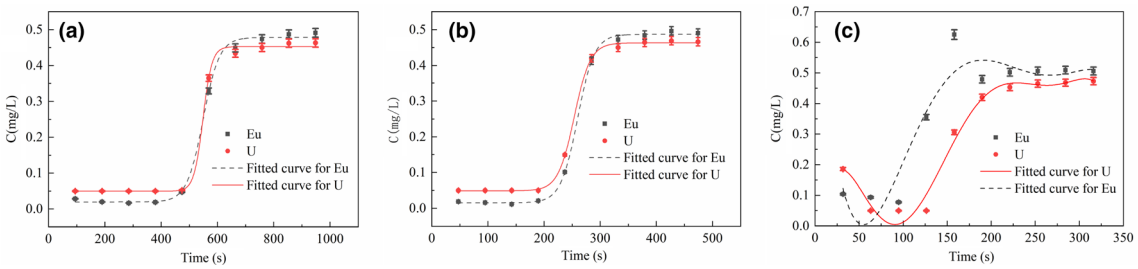

Fig. 7 (Color online) Plots of the separation of uranium and europium mixed solutions at different sample flow rates. **a** sample flow rate of 1.908 mL/min; **b** sample flow rate of 3.802 mL/min; **c** sample flow rate of 5.698 mL/min

3.1.3 Effect of sample injection flow rate on the separation of uranium and europium

The sample flow rate could control the ion separation time and improved the maneuverability of nuclide ion separation. Therefore, the choice of sample flow rate was highly important; a speed too slow or too fast could lead to difficulty in the separation of nuclide ions. Experimentally, 30 mL of a mixed solution of uranium and europium at pH = 2 was used for separation sampling; one sample was taken every 3 mL and subsequently detected by ICP-OES. The results of this are shown for different sample flow rates in Fig. 7. The sample flow rate shown in Fig. 7a was 1.908 mL/min, at which, the separation of the column for the mixed nuclides was the least effective, and separation only began at the 7th set of samples. The sample flow rate shown in Fig. 7b was 3.802 mL/min; at this flow rate, the separation of the mixed solution began from the 6th set of samples. The sample flow rate shown in Fig. 7c was 5.698 mL/min; at this sample flow rate, the separation of uranium and europium was optimal, with separation of uranium and europium starting at the 4th set of samples, and the best separation time point being approximately 150 s.

Achieving a larger separation factor and fewer separation stages were the objectives of the experimental study. The separation factor could be obtained theoretically through preliminary experiments, and the separation stages were obtained by the following equation:

$$ab^n = c\ , \tag{1}$$

where a is the ratio of the concentration of uranium in the initial solution to the concentration of the major coexisting ions (e.g., europium or sodium ions); b is the separation factor, which can be calculated experimentally; n is the number of stages of separation, and c is the ratio of the concentration of uranium in the solution after separation to the concentration of the major coexisting ions.

As shown in Fig. 7c, the separation factor of uranium and europium was 1.088 at a sample flow rate of 5.698 mL/min. According to Eq. (1), the initial separation of uranium and europium from the solution was calculated at more than 47 times. Therefore, the sample flow rate of the column during the experiment was set at 5.698 mL/min.

3.1.4 Effect of column heating temperature on the separation of uranium, europium, and sodium ions

Heating and cooling during the chromatographic column path can have the effect of "slowing down" and "speeding up" the ions, which can help to further achieve separation of

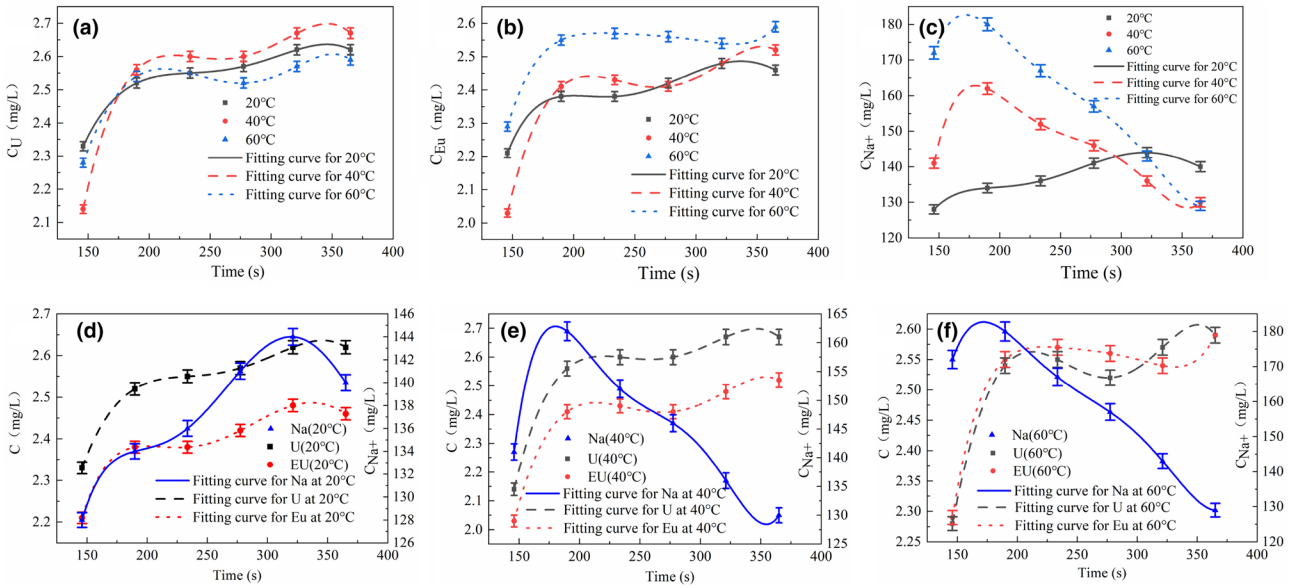

Fig. 8 (Color online) Separation of each element in the mixed solution at different temperatures. **a** Separation of uranyl ions in the mixed solution at different temperatures; **b** Separation of europium ions in the mixed solution at different temperatures; **c** Separation of sodium ions in the mixed solution at different temperatures; **d**, **e** and **f** represent the separation of the three ions in the mixed solution at 20 ℃, 40 ℃ and 60 ℃

nuclide ions. The heating and cooling paths of the column were divided into five stages according to column length, while cooling bath temperature was fixed at 15 ℃. The separation of a mixture of uranium, europium, and sodium ions from the column in a heating bath at 20, 40, and 60 ℃ was investigated at pH = 2 and at a sample flow rate of 5.698 mL/min. A mixture of 25 mL of uranium, europium, and sodium ions was added to the column for separation, in which the concentrations of uranium and europium were the same. The last 18 mL of sample exiting the column, one sample for every 3 mL of solution, was collected and analyzed, as shown in Fig. 8. Figure 8a shows the separation of uranyl ions in the mixed solution at different temperatures, and it can be seen here that uranyl ions had the highest concentration after exiting the column at the same time ($t > 180$ s) at 40 °C, i.e., the best separation concentration, while 60 ℃ was the lowest. Figure 8b shows the separation of europium ions in the mixed solution at different temperatures, and the concentration of europium ions exiting the column increased with an increase in temperature. Figure 8c shows the separation of sodium ions in the mixed solution at different temperatures. The separation of sodium ions also increased with increasing temperature.

Figure 8d shows the separation of the three mixed elements at a column temperature of 20 ℃. The separation curves for uranium, europium, and sodium ions were essentially the same at 20 ℃. The separation of uranium and sodium ions was relatively poor in the separation solution exiting the column before 300 s, although the separation was good after 300 s, when the concentrations of uranium and sodium ions exiting the column showed high variation. Figure 8e shows the separation of the three mixed elements at a column temperature of 40 ℃. The separation of uranium and europium and uranium and sodium ions was good at 40 ℃, particularly after 300 s, when the difference in concentration between uranium and sodium ions was the largest. Furthermore, the separation factor of uranium and europium under this condition was 1.088. Figure 8f shows the separation of the three mixed elements at a column temperature of 60 ℃. The separation of europium and uranium at 60 ℃ was poor, while the difference in concentration between the two elements after separation was not significant, although the separation of uranium and sodium was greatest after 300 s. In Fig. 8 d, e and f, the separation factors of uranium and sodium were 1.037 at 20 ℃, 1.0567 at 40 ℃, and 1.0809 at 60 ℃. These figures showed that the separation of uranium and europium was best under low-temperature conditions, while separation of uranium and sodium ions was the worst. The separation of uranium and europium was the worst under high-temperature conditions, although this was when the separation factor of uranium and sodium ions was the highest. The main reason for this was that the ionic motion states of light and heavy ions were slower under low-temperature conditions, and after the light and heavy ions were blocked by the separation unit inside the column, the motion rate did not change significantly. The concentration of sodium ions in the back-end solution was therefore higher, so the separation effect of sodium ions and uranium was

poor. At higher temperatures, the light ions were more active than the heavy ions, so the sodium ions could pass through the separation unit layer more easily while the sodium ions moved at a faster rate and exited the column first. Therefore, the latter part of the separation solution had a lower sodium ion content with a higher uranium content, which could better achieve the separation of uranium and sodium ions. However, as a result of the small mass difference between uranium and europium ions, the temperature increased, and the ions were therefore more likely to collide and intermingle when passing through the separation unit, leading to a lower separation effect. In summary, the heating temperature of the column for the seawater uranium extraction experiment was chosen to be 60 °C.

3.1.5 Effect of sodium ions on the separation of uranium and europium

The cations in seawater are more complex, and the separation of uranium in the column under different cation environments was experimentally studied, as shown in Fig. 9, whereby 1 mL of varying concentrations of cations was added to 20 ml of uranium and europium mixed solution. Figure 9a shows the separation of uranium and europium after adding 1 mL of 1 mol/L sodium ions. The separation time of the mixed solution coming out from the column was between 100 and 200 s, with the concentration difference between uranium and europium being the largest, and having the greatest separation. In addition, the concentration of europium in the separation solution exiting the column was constantly higher than that of uranium. Figure 9b shows the separation of uranium and europium after adding 1 mL of 0.5 mol/L sodium ions, which was higher than that of uranium before 125 s, while the concentration of europium was higher than that of uranium after 125 s. Furthermore, the best separation time of uranium and europium was after 200 s. Figure 9c shows the separation of uranium and europium after adding 1 mL of 0.1 mol/L sodium ions, and the concentration of uranium in the separation solution from the column was clearly higher than that of europium. The concentration difference between uranium and europium was larger and the separation effect was better in this case. Comparing the three plots in Figs. 9 a, b and c, the separation of uranium and europium on the column was greatest between 125 and 200 s when 1 mol/L sodium ions was added. After 200 s, the concentration of sodium ions in the mixed solution had little effect on the separation of uranium and europium.

3.2 Separation of uranium and sodium ions in water samples from the Ganjiang River

By studying the performance of the chromatographic column, the separation of uranium and other nuclide ions could be achieved after a mixed solution of uranium, europium, and sodium ions was separated by the column. Therefore, to further verify the feasibility of this device, experiments were conducted on water samples from the Ganjiang River to determine the concentration ratio of separated uranium and sodium ions in the water samples. A 20 L water sample from the Ganjiang River was evaporated and then concentrated to 2 L. The pH of this 2 L water sample was subsequently adjusted to 2. The sample feed flow rate was set at 5.698 mL/min. The chromatographic column was heated to 60 °C and then cooled to 15 °C, for five cycles between hot and cold in this way. The parameters of the pulse injection device were set as follows: $T_1 = 70$ s, $T_2 = 200$ s, $T_3 = 220$ s, where T_1 is the air pulse time, T_2 is the pulse injection time (Injection volume is 20 ml), and T_3 is the optimum separation time after the sample was removed from the column. According to Fig. (8), the optimal separation point for uranium and sodium ions was at around 220 s (15 mL) for each 20 mL sample injection, therefore the first 15 mL of separation was collected experimentally. Pulsed injection separation was then performed according to these optimum separation conditions, and the sample solution collected from the separation was subjected to the next stage of separation for four

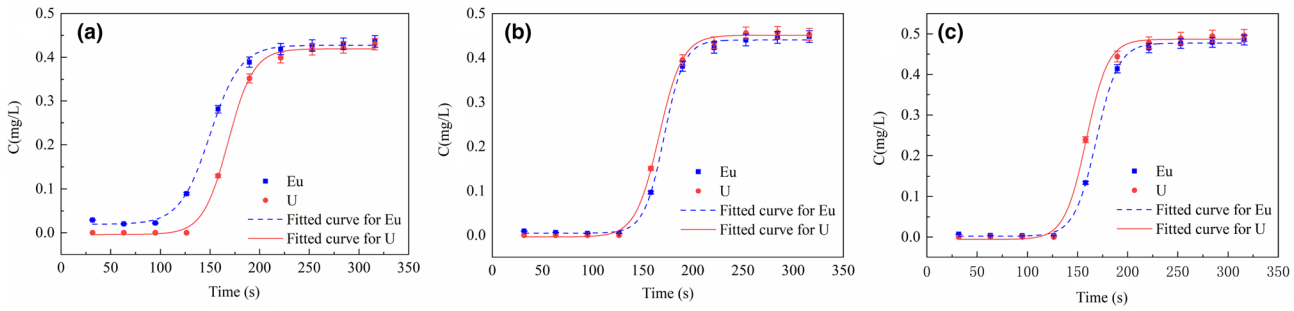

Fig. 9 (Color online) Diagram of the separation of mixed solutions of uranium, europium and sodium ions. 1 mL, 1 mol/L of sodium ion was added to the mixed solution of uranium and europium (**a**); 1 mL, 0.5 mol/L of sodium ion was added to the mixed solution of uranium and europium (**b**); 1 mL, 0.1 mol/L of sodium ion was added to the mixed solution of uranium and europium (**c**)

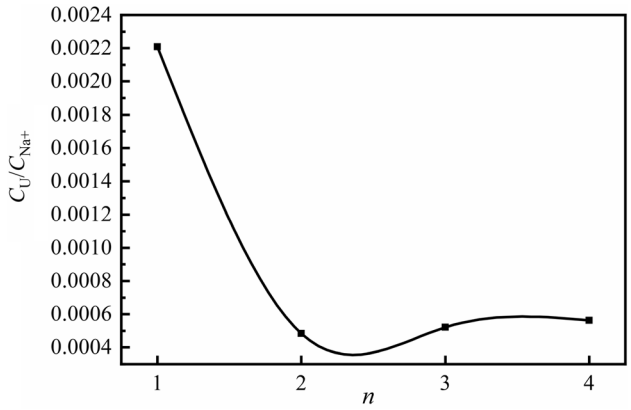

Fig. 10 Determination of uranium-sodium ion concentration ratio in the separation front-end liquid of in water samples from the Ganjiang River after separation

stages. The uranium to sodium ion concentration ratio was then determined for each stage of the sample, with the experimental results for this being shown in Fig. 10. These results showed that the uranium–sodium ion concentration ratio in the front-end liquid of the first separation stage was 0.0022, while the uranium–sodium ion concentration ratio after the 4th separation was 0.00056. Therefore, the uranium–sodium ion concentration ratio after the first separation was 3.93 times higher than that after the 4th separation, indicating that the sodium ion concentration in the front-end liquid of the separation increased continuously while the uranium concentration decreased continuously with the increase in separation stages. In other words, the separation front-end solution was enriched with sodium ions. Conversely, the separation back-end solution is the separation enrichment of uranium.

The experimental results showed that the water sample in the Ganjiang River could separate uranium and sodium ions after entering the column using pulsed feed. According to Eq. (1), the separation factor of uranium and sodium was calculated to be 1.50, and more than 21 stages were theoretically required to achieve the initial separation of uranium and sodium.

3.3 Study on uranium extraction from seawater

The separation of water samples from the Ganjiang River further validated the feasibility and scientific validity of the pulsed liquid chromatography separation method, which was designed to allow for the separation and extraction of uranium from seawater in complex environments. Therefore, 20 L of seawater was taken (from Xiamen, Fujian Province) for the experiment and the samples were pretreated according to the optimum separation conditions, followed by a pulsed injection separation. The experimental conditions were the same as those used for the separation of the water samples from the Ganjiang River. The parameters of the pulsed injection device were set, where the parameters are the same as in Sect. 3.2 of the text, and 20 mL of the sample was then pulsed into the column each time. The first 15 mL of the solution from the

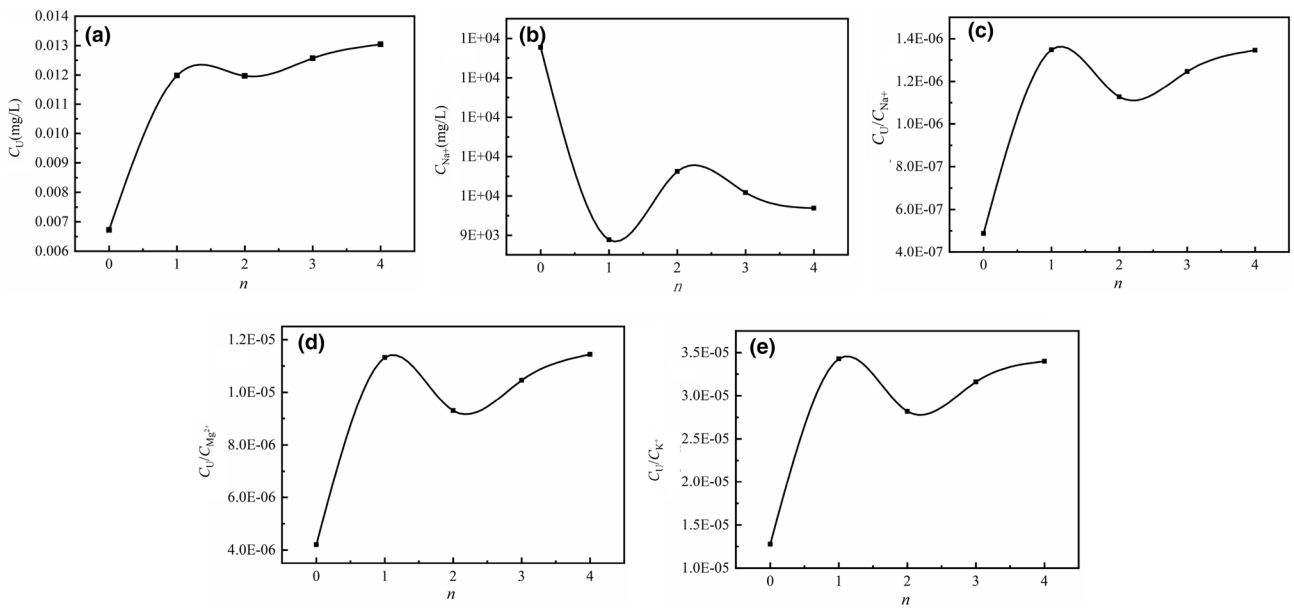

Fig. 11 Changes in ion concentrations in the separation solution after four stages of separation of the original sample of seawater at pH = 2. Changes of uranium concentration after separation of four stages (**a**); separation of sodium ions in seawater (**b**); concentration ratio of uranium and sodium ions in seawater at different separation stages (**c**); concentration ratio of uranium and magnesium ions in seawater at different separation stages (**d**); concentration ratio of uranium and potassium ions in seawater at different separation stages (**e**)

Table 2 Standard analysis of elements to be measured in seawater samples by ICP-MS using KED mode

Elements	Linear equation	R^2	LOD (ppb)	BEC (ppb)
U	$f(x) = 170{,}484.2193x + 107.3543$	0.9999	0.0018	0.001
Na	$f(x) = 1048.2703x + 7591.6695$	0.9998	0.3925	7.242
Mg	$f(x) = 488.2858x + 139.3347$	0.9997	0.0741	0.285
K	$f(x) = 396.1091x + 7906.5578$	0.9998	1.1170	19.961

column was used as the front-end solution and was refluxed into the primary cuvette. The final 5 mL of the solution was subsequently collected as the back-end enrichment solution. All 20 L of seawater were separated once for one stage, and the collected back-end solution was then separated for the next stage, with a total of four stages being separated in the experiment. The variations in uranium, sodium, magnesium, and potassium ion concentrations in the seawater samples were determined using ICP-MS, with the results of this being shown in Fig. 11. Table 2 presents an analysis of the corresponding standard substances for each element.

Figure 11a shows the variation in uranium concentration in the back-end enrichment solution for the four stages of seawater separation, while Fig. 11b shows the variation in sodium ion concentration in the back-end solution for the four stages of seawater separation. These results showed that the concentration of uranium continued to increase while the concentration of sodium ions continued to decrease as the number of separation stages increases. The initial concentration of uranium in seawater measured in Fig. 11a was 6 μg/L, higher than that of normal seawater (3.3 μg/L). This was mainly because the experiment first used nitric acid to adjust the pH of the 20 L seawater samples to 2 during the pretreatment of seawater to prevent deterioration A vacuum pump was then used to filter the seawater to remove solid impurities. However, the pores of the Brinell funnel used for filtration contained residues from the previous filtration, which could not be cleaned off when the funnel was cleaned using low acid or distilled water. The seawater sample to be removed was adjusted to pH = 2 using strong nitric acid, so that the seawater sample passed through the funnel at low pH and washed the uranium from the residue into the sample, resulting in an increase in uranium concentration. Figure 11 c shows the ratios of uranium and sodium ion concentrations for the four separation stages. The ratio of uranium and sodium ion concentrations in the original seawater sample was 4.883×10^{-7}, while the ratio of uranium and sodium ion concentrations after the separation of the 4th stage was 1.346×10^{-6}. According to the calculation formula (1) for the number of separation stages, the separation factor of uranium and sodium ions in seawater was $b = 1.2885$, and the separation of uranium and sodium ions in seawater was successful. Theoretically, 28 stages were required for this. Figure 11 d shows the ratio of uranium and magnesium ion concentrations for the four stages of separation. The ratio of uranium and magnesium ion concentrations in the original seawater sample was 4.206×10^{-6}, while the ratio of uranium and magnesium ion concentrations after the fourth stage of separation was 1.144×10^{-5}, 2.72 times that of the initial sample. Furthermore, the separation factor of uranium and magnesium ions in seawater was $b = 1.2847$. Figure 11e then shows the ratios of the uranium and potassium ion concentrations for the four stages of separation. The ratio of uranium and potassium ion concentrations in the original seawater sample was 1.276×10^{-5}, and the ratio of uranium and potassium ion concentrations after the fourth stage of separation was 3.398×10^{-5}. Additionally, the separation factor of uranium and potassium ions in seawater was $b = 1.2773$. The main cations were sodium, magnesium, and potassium ions. The separation factors of these three ions and uranium were all similar, while also being relatively large. Furthermore, a lower number of stages was required to separate uranium from these three cations, therefore, theoretically, after 28 stages of seawater sample separation, uranium solution could be extracted from the seawater. After experimental verification, this new pulsed liquid chromatography radionuclide separation method could be applied to seawater uranium extraction, and was more effective for the separation of uranium and sodium ions in seawater with high selectivity.

3.4 Study on separation mechanism

The retention time of uranyl ions in the column is defined as the time from when the aqueous solution flows to the "time-controlled automatic shunt system" to when the uranyl ions start to appear here. The duration of this depends on the flow rate, pH, filling particle size, coexisting ion strength, tube diameter, temperature, and other factors. Under the same conditions, the retention times of different ions were different. The average retention time of the ions is calculated from Eq. (2).

$$\text{Average retention time}(t) = \text{Retention time}(T)/\text{Total number of separation units}(n_0), \quad (2)$$

where t is the average retention time, T is the retention time, and n_0 is the total number of separated units.

Retained liquid film: When a solid is removed from the liquid that can wet it, the liquid film attached to the surface is

called the retained liquid film. The most important physical quantity of this is the thickness, d. If the liquid film thickness of the column filling is the same as the liquid film thickness of the tube wall, the retained liquid film thickness of each filling in the column is given by Eqs. (3) and (4).

$$\frac{V_1}{\text{separation units} \times Z} + V_x = \frac{4\pi}{3}\left(d + r_x\right)^3, \tag{3}$$

$$V_2 - \left(V_0 - V_1\right) = \pi \times L \times \left(r_2 - d\right)^2, \tag{4}$$

where d is the thickness of the retained liquid film per filling, V_0 is the total volume of the retained liquid film inside the column (mm^3), V_1 is the volume of the liquid film on the filling (mm^3), V_x is the volume of each filling (mm^3), V_2 is the volume of the internal space of the column (mm^3), Z is the number of particles of the filling on each separation unit, r_x is the radius of each filling (0.5 mm), r_2 is the column inner cavity half-warp (1.5 cm), and L is the column length (10 m). V_0 can be measured experimentally, while V_x, r_x, and Z are related to the selected filling particle size; and V_2, r_2, and L are related to the required chromatographic column tube. The liquid film thickness d per filler was 38.02 μm in this study.

Non-equilibrium kinetics: Considering that the filling particle size was much larger than the nuclide ions and that its concentration change was negligible, this interaction could be regarded as a first-order reaction and the first order kinetic equation for the interaction rate of nucleophile ions with the packing is derived as in Eq. (5).

$$r = \frac{\mathrm{d}x}{\mathrm{d}t} = k(a - x), \tag{5}$$

where r is the rate of ion-filler interaction (mg/L), a is the concentration of ions in the packed liquid film at the initial time (mg/L), x is the concentration of ions in the filling liquid film at time t (mg/L), t is the interaction time (average retention time), and k is the reaction rate constant. Since the rate of interaction r and average retention time t can be obtained through macroscopic experiments, the change in ion motion of the liquid membrane of each separation unit could be calculated.

From the previous experimental data, it can be observed that when pH > 6, most of the uranyl ions were adsorbed on the surface of the filling, both within the surface liquid film of the filling; when 2 < pH < 6, some of the uranyl ions were adsorbed on the surface of the filling and reached relative equilibrium as a result. Furthermore, when pH < 2, the ions were in non-equilibrium with the filling, as shown in Fig. 12.

The non-equilibrium separation mechanism of pulsed liquid chromatography nuclide separation method was as follows: The ions to be separated (aqueous phase containing uranium and other impurity ions at pH = 2) interacted with

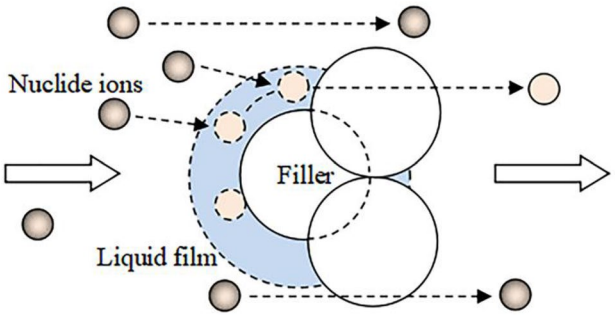

Fig. 12 (Color online) Schematic diagram of the non-equilibrium state interaction of nuclide ions with filling

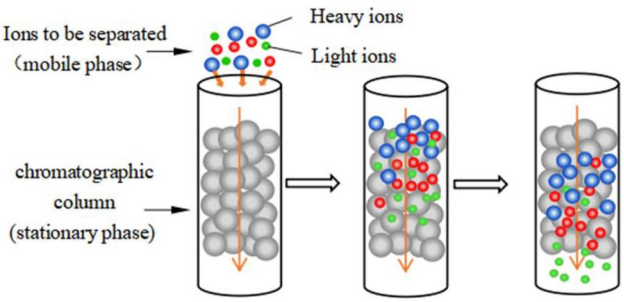

Fig.13 (Color online) Schematic diagram of the separation mechanism of the chromatographic column

the column filling (stationary phase), and the dynamic separation of ions could be carried out because of the different forces between different ions and the column, the different average retention times of the ions, and the different accelerations of the forces on ions. The light and low-valence ions were subjected to the small blocking effect of the column and flowed out from the column first, while the heavy particles and high-valence ions were subjected to the large blocking effect of the column and therefore flowed out from the column later, so as to achieve the separation of light and heavy particles. This separation mechanism of nuclides is shown in Fig. 13. Using the separation mechanism of the new column, the average retention time of the nuclides in the column was studied, and the separation between different nuclide ions could be improved by changing the average retention time of different nuclides in the column. The separation enrichment of the target nuclides and other nuclide ions at different time periods was also analyzed and determined. A pulsed feed separation device was used to selectively separate and collect the enrichment of target nuclides at different time periods. This pulsed injection method was key to the separation method, which used a "one-by-one" injection method to achieve segmented and graded separation and extraction of uranium in a pulsed discontinuous manner. This segmented method intercepted the target

nuclide according to the separation of different nuclides in the column; the graded method re-entered the column for the segmented separation of the intercepted target nuclide. Using this method to separate and extract uranium from seawater, sodium ions belonged to light ions and low valence ions, therefore the sample solution exited out the front end with a high sodium ion content after separation from the column, while uranium ions in seawater belonged to heavy particles and high valence ions. The latter part of the sample solution coming out of the column contained a high uranium concentration, and each time the pulse feed was separated, the latter part of the sample solution was collected, and the enriched solution was then repeatedly separated by pulse feed to realize uranium extraction from seawater.

4 Conclusion

The new pulsed liquid chromatography method proposed here was able to solve the problem of continuous injection in traditional chromatographic separation, and realized the rapid, efficient, and low-cost separation of uranium and other elements in water, while also achieving the stepwise and graded separation and extraction of uranium in a pulsed discontinuous manner. The separation of uranium was investigated at different pH over-column acidities, sample injection flow rates, column heating temperatures, and cation systems. The experimental study for each condition tentatively determined that this method could be used for the separation of uranium and other ions (europium and sodium ions), while the optimal conditions for the separation of uranium and sodium ions were also obtained here. Based on analysis of the experimental data for each condition, the formulae for the number of separation stages required to achieve separation by the method were derived. The separation of uranium and sodium ions was performed using samples from the Ganjiang River under these optimal separation conditions, with a separation factor of 1.50 given for uranium and sodium ions, which would theoretically require 21 stages to achieve the separation of uranium and sodium. Overall, these experiments demonstrated the feasibility of this pulsed liquid chromatography separation method. Finally, preliminary separation experiments were also conducted for uranium, sodium, magnesium, and potassium ions in seawater samples. Subsequently, their separation factors were obtained, in which the separation factor of uranium and sodium ions was 1.2885, suggesting that the complete separation of uranium and sodium ions in seawater would require more than 28 stages. As the most abundant ions in seawater, sodium ions can theoretically separate uranium from other impurity ions if the separation of uranium and sodium ions is achieved, meaning that, after 28 stages of seawater separation, uranium can be extracted from seawater. Through a preliminary separation study on seawater samples, it was determined that our pulsed liquid chromatography separation method could be applied in seawater uranium extraction studies. The pulsed liquid chromatography method presented in this study is innovative and feasible regarding the separation and enrichment of nuclides while providing new ideas for the study of uranium extraction from seawater.

Author contributions All authors contributed to the study conception and design. Material preparation, data collection and analysis were performed by Jian-Hua Ye and Tao Yu. The first draft of the manuscript was written by Jian-Hua Ye and all authors commented on previous versions of the manuscript. All authors read and approved the final manuscript.

References

1. R.R. Alnuaimi, B. Khuwaileh, M. Zubair et al., Nuclear design of an integrated small modular reactor based on the APR-1400 for RO desalination purposes. Nucl. Sci. Tech. **33**, 95 (2022). https://doi.org/10.1007/s41365-022-01082-2
2. H.B. Yang, X.Q. Li, Y.H. Yu et al., Design and evaluation of prototype readout electronics for nuclide detector in very large area space telescope. Nucl. Sci. Tech. **33**, 65 (2022). https://doi.org/10.1007/s41365-022-01047-5
3. C.W. Abney, R.T. Mayes, T. Saito et al., Materials for the recovery of uranium from seawater. Chem. Rev. **117**, 13935–14013 (2017). https://doi.org/10.1021/acs.chemrev.7b00355
4. Y.F. Yue, R.T. Mayes, J.S. Kim et al., Seawater uranium sorbents: preparation from a mesoporous copolymer initiator by atom-transfer radical polymerization. Angew. Chem. Int. Ed. **52**, 13458–13462 (2013). https://doi.org/10.1002/anie.201307825
5. Y.D. Pu, T.T. Qiang, L.F. Ren, Waste feather fibre based high extraction capacity bio-adsorbent for sustainable uranium extraction from seawater. Int. J. Biol. Macromol. **206**, 699–707 (2022). https://doi.org/10.1016/j.ijbiomac.2022.03.019
6. G. Cheng, A.R. Zhang, Z.W. Zhao et al., Extremely stable amidoxime functionalized covalent organic frameworks for uranium extraction from seawater with high efficiency and selectivity. Sci. Bull. **66**(19), 1994–2001 (2021). https://doi.org/10.1016/J.SCIB.2021.05.012
7. H. Guo, P. Mei, J.T. Xiao et al., Carbon materials for extraction of uranium from seawater. Chemosphere **278**, 130411 (2021). https://doi.org/10.1016/J.CHEMOSPHERE.2021.130411
8. Y.D. Pu, T.T. Qiang, L.F. Ren, Anti-biofouling bio-adsorbent with ultrahigh uranium extraction capacity: one uranium resource recycling solution. Desalination **531**, 115721 (2022). https://doi.org/10.1016/J.DESAL.2022.115721
9. P.H. Ju, K.T. Alali, G.H. Sun et al., Swollen-layer constructed with polyamine on the surface of nano-polyacrylonitrile cloth used for extract uranium from seawater. Chemosphere **271**, 129548 (2021). https://doi.org/10.1016/J.CHEMOSPHERE.2021.129548
10. S. Das, A.K. Pandey, A. Athawale et al., Exchanges of uranium(VI) species in amidoxime-functionalized sorbents. J. Phys. Chem. **113**(18), 6328–6335 (2009). https://doi.org/10.1021/jp8097928
11. H. Li, S. Wang, Reaction: semiconducting MOFs offer new strategy for uranium extraction from seawater. Chem. Rev. **7**(2), 279–280 (2021). https://doi.org/10.1016/J.CHEMPR.2021.01.013
12. Y.D. Wu, W.R. Cui, C.R. Zhang et al., Regenerable, anti-biofouling covalent organic frameworks for monitoring and extraction of

uranium from seawater. Environ. Chem. **19**, 1847–1856 (2021). https://doi.org/10.1007/S10311-020-01179-3
13. B. Yan, C. Ma, J. Gao et al., An lon-crossiinked supramolecular hydrogel for ultrahigh and fast uranium recovery from seawater. Adv. Mater. **32**(10), 1906615 (2020). https://doi.org/10.1002/adma.201906615
14. Z.Y. Bai, Q. Liu, H.S. Zhang et al., Mussel-inspired anti-biofouling and robust hybrid nanocomposite hydrogel for uranium extraction from seawater. J. Hazard. Mater. **381**, 120984 (2019). https://doi.org/10.1016/j.jhazmat.2019.120984
15. Z.Y. Wang, Q.Y. Meng, R.C. Ma et al., Constructing an ion pathway for uranium extraction from seawater. Chem **6**(7), 1683–1691 (2020). https://doi.org/10.1016/j.chempr.2020.04.012
16. A.F. Ismail, M.S. Yim, Investigation of activated carbon adsorbent electrode for electrosorption-based uranium extraction from seawater. Nucl. Eng. Technol. **47**(5), 579–587 (2015). https://doi.org/10.1016/j.net.2015.02.002
17. C. Liu, P.C. Hsu, J. Xie et al., A half-wave rectified alternating current electrochemical method for uranium extraction from seawater. Nat. Energy **2**(4), 294–303 (2017). https://doi.org/10.1038/nenergy.2017.7
18. C.X. Dong, T.T. Qiao, Y.B. Huang et al., Efficient photocatalytic extraction of uranium over ethylenediamine capped cadmium sulfide telluride nanobelts. ACS Appl. Mater. Interfaces **13**(10), 11968–11976 (2021). https://doi.org/10.1021/acsami.0c22800
19. M.W. Chen, T. Liu, X.B. Zhang et al., Photoinduced enhancement of uranium extraction from seawater by MOF/black phosphorus quantum dots heterojunction anchored on cellulose nanofiber aerogel. Adv. Funct. Mater. **31**(22), 2100106 (2021). https://doi.org/10.1002/adfm.202100106
20. K. Lin, W.Y. Sun, L.J. Feng et al., Kelp inspired bio-hydrogel with high antibiofouling activity and super-toughness for ultrafast uranium extraction from seawater. Chem. Eng. J. **430**, 133121 (2021). https://doi.org/10.1016/J.CEJ.2021.133121
21. S. Yang, Y. Cao, T. Wang et al., Positively charged conjugated microporous polymers with antibiofouling activity for ultrafast and highly selective uranium extraction from seawater. Environ. Res. **183**, 109214 (2020). https://doi.org/10.1016/j.envres.2020.109214
22. S. Das, A.K. Pandey, A. Athawale et al., Chemical aspects of uranium recovery from seawater by amidoximated electron-beam-grafted polypropylene membranes. Desalination **232**(1–3), 243–253 (2008). https://doi.org/10.1016/j.desal.2007.09.019
23. S. Das, Z.Y. Wang, B. Suree et al., Strategies toward the synthesis of advanced functional sorbent performance for uranium uptake from seawater. Ind. Eng. Chem. Res. **60**, 15037–15044 (2021). https://doi.org/10.1021/ACS.IECR.1C02920
24. S. Abdel, I. Fatma et al., Synthesis of gemini cationic surfactant for proficient extraction of uranium (VI) from sulfuric acid solution. J. Radioanal. Nucl. Chem. **330**, 175–189 (2021). https://doi.org/10.1007/s10967-021-07966-8
25. S. Shi, B.C. Li, Y.X. Qian et al., A simple and universal strategy to construct robust and anti-biofouling amidoxime aerogels for enhanced uranium extraction from seawater. Chem. Eng. J. **397**, 125337 (2020). https://doi.org/10.1016/j.cej.2020.125337
26. Y. Wang, Y.P. Zhang, Q. Li et al., Amidoximated cellulose fiber membrane for uranium extraction from simulated seawater. Carbohydr. Polym. **245**(2), 116627 (2020). https://doi.org/10.1016/j.carbpol.2020.116627
27. Y. Wang, Z.W. Lin, H.S. Zhang et al., Anti-bacterial and superhydrophilic bamboo charcoal with amidoxime modified for efficient and selective uranium extraction from seawater. J. Colloid. Interface Sci. **598**, 455–463 (2021). https://doi.org/10.1016/J.JCIS.2021.03.154
28. L.S. Yang, H.C. Xiao, Y.C. Qian et al., Bioinspired hierarchical porous membrane for efficient uranium extraction from seawater. Nat. Sustain. **5**(1), 71–80 (2021). https://doi.org/10.1038/S41893-021-00792-6.5(1)
29. P.P. Mei, R. Wu, S. Shi et al., Conjugating hyaluronic acid with porous biomass to construct anti-adhesive sponges for rapid uranium extraction from seawater. Chem. Eng. J. **420**, 130382 (2021). https://doi.org/10.1016/J.CEJ.2021.130382
30. M. Wehbie, G. Arrachart, T. Sukhbaatar et al., Extraction of uranium from sulfuric acid media using amino-diamide extractants. Hydrometallurgy **200**(23), 105550 (2020). https://doi.org/10.1016/J.HYDROMET.2020.105550
31. Z. Zhang, F. Yong, L. Zhang et al., High performance task-specific ionic liquid in uranium extraction endowed with negatively charged effect. J. Mol. Liq. **336**, 116601 (2021). https://doi.org/10.1016/J.MOLLIQ.2021.116601
32. R.H. Yan, W.R. Cui, C.R. Zhang et al., Bio-inspired hydroxylation imidazole linked covalent organic polymers for uranium extraction from aqueous phases-sciencedirect. Chem. Eng. J. **420**, 129658 (2021). https://doi.org/10.1016/J.CEJ.2021.129658
33. Z. Ahmad, Y. Lia, J.J. Yang et al., A membrane-supported bifunctional poly(amidoxime-ethyleneimine) network for enhanced uranium extraction from seawater and wastewater. J. Hazard. Mater. **425**, 127995 (2021). https://doi.org/10.1016/J.JHAZMAT.2021.127995
34. J.W. Wang, Y. Sun, X.M. Zhao et al., A poly(amidoxime)-modified mof macroporous membrane for high-efficient uranium extraction from seawater. E-Polym. **22**(1), 399–410 (2022). https://doi.org/10.1515/EPOLY-2022-0038
35. P. Li, J.J. Wang, W. Yun et al., Photoconversion of U(VI) by TiO2: an efficient strategy for seawater uranium extraction. Chem. Eng. J. **365**, 231–241 (2019). https://doi.org/10.1016/j.cej.2019.02.013
36. Y. Wang, J.J. Wang, J. Wang et al., Efficient recovery of uranium from saline lake brine through photocatalytic reduction. J. Mol. Liq. **308**, 113007 (2020). https://doi.org/10.1016/j.molliq.2020.113007
37. F.T. Yu, Z.Q. Zhu, S.P. Wang et al., Tunable perylene-based donor-acceptor conjugated microporous polymer to significantly enhance photocatalytic uranium extraction from seawater. Chem. Eng. J. **412**, 127558 (2020). https://doi.org/10.1016/j.cej.2020.127558
38. X. Zhong, Y.X. Liu, T. Hou et al., Effect of Bi2 WO6 nanoflowers on the U(VI) removal from water: roles of adsorption and photoreduction. J. Environ. Chem. Eng. **10**, 107170 (2022). https://doi.org/10.1016/J.JECE.2022.107170
39. K.D. Zhou, Y.C. Ding, L.F. Zhang et al., Synthesis of mesoporous ZnO/TiO_2-SiO_2 composite material and its application in photocatalytic adsorption desulfurization without the addition of an extra oxidant. Dalton. Trans. **49**(5), 1600–1612 (2020). https://doi.org/10.1039/C9DT04454J
40. P. Li, Y. Wang, J.J. Wang et al., Carboxyl groups on g-c3n4 for boosting the photocatalytic u(vi) reduction in the presence of carbonates. Chem. Eng. J. **414**(28), 128810 (2021). https://doi.org/10.1016/J.CEJ.2021.128810
41. K. Chen, C.L. Chen, X.M. Ren et al., Interaction mechanism between different facet tio2 and U(VI): experimental and density-functional theory investigation. Chem. Eng. J. **359**, 944–954 (2018). https://doi.org/10.1016/j.cej.2018.11.092
42. J. Lei, H.H. Liu, F.C. Wen et al., Tellurium nanowires wrapped by surface oxidized tin disulfide nanosheets achieves efficient photocatalytic reduction of U(VI). Chem. Eng. J. **426**, 130756 (2021). https://doi.org/10.1016/J.CEJ.2021.130756
43. P.L. Liang, L.Y. Yuan, H. Deng et al., Photocatalytic reduction of uranium(VI) by magnetic $ZnFe_2O_4$ under visible light. Appl. Catal. B Environ. **267**, 118688 (2020). https://doi.org/10.1016/j.apcatb.2020.118688
44. J. Chen, Z.J. Gong, W.Y. Tang et al., Carbon dots in sample preparation and chromatographic separation: recent advances and future

prospects. Trends. Analyt. Chem. **134**, 116135 (2020). https://doi.org/10.1016/J.TRAC.2020.116135
45. X.Z. Li, Q.X. Zhang, H.Y. Tan et al., Fast nuclide identification based on a sequential bayesian method. Nucl. Sci. Tech. **32**, 143 (2021). https://doi.org/10.1007/s41365-021-00982-z
46. L. Chen, R. Yan, X.Z. Kang et al., Study on the production characteristics of ^{131}I and ^{90}Sr isotopes in a molten salt reactor. Nucl. Sci. Tech. **32**, 33 (2021). https://doi.org/10.1007/s41365-021-00867-1